Analysis of the PM$_{2.5}$–O$_3$ Pollution Characteristics and Its Potential Sources in Major Cities in the Central Plains Urban Agglomeration from 2014 to 2020

Shu Quan [1], Miaohan Liu [1], Boxuan Chen [1], Yuehua Huang [2], Meijuan Wang [3], Qingxia Ma [4] and Yan Han [1,*]

[1] College of Geography and Environmental Science, Henan University, Kaifeng 475004, China
[2] School of Atmospheric Sciences, Nanjing University of Information Science and Technology, Nanjing 210044, China
[3] Kaifeng Weather Bureau, Kaifeng 475004, China
[4] Henan University Integrated Prevention and Control of Air Pollution and Ecological Safety Key Lab of Henan, Kaifeng 475004, China
[*] Correspondence: hanyanhd@163.com

Abstract: To highlight the characteristics of PM$_{2.5}$–O$_3$ pollution in the Central Plains Urban Agglomeration, spatial and temporal characteristics, key meteorological factors, and source pollution data for the area were analyzed. These data from the period 2014–2020 were obtained from state-controlled environmental monitoring stations in seven major cities of the agglomeration. The results revealed the following: (1) Spatially, the PM$_{2.5}$–O$_3$ pollution days were aggregated in the central area of Xinxiang and decreased toward the north and south. Temporally, during the 2014–2020 period, 50 days of PM$_{2.5}$–O$_3$ pollution were observed in the major cities of the Central Plains Urban Agglomeration, with an overall decreasing trend. (2) A low-temperature, high-pressure environment appeared unfavorable for the occurrence of PM$_{2.5}$–O$_3$ pollution days. Wind speeds of 2.14–2.19 m/s and a southerly direction increased the incidence of PM$_{2.5}$–O$_3$ pollution days. (3) The external transport range in summer was smaller and mainly originated from within Henan Province. These results can provide important reference information for achieving a synergistic control of PM$_{2.5}$–O$_3$ pollution, determining the meteorological causes, as well as the potential sources, of PM$_{2.5}$–O$_3$ pollution in polluted areas and promoting air pollution control.

Keywords: spatial variation; temporal variation; meteorological factors; potential source analysis; Henan province

1. Introduction

Air pollution is a major environmental concern worldwide, which is being exacerbated by rapid urbanization and other anthropogenic activities [1–3]. In recent years, to control and minimize air pollution, varying measures have been implemented in different countries [4–6]. However, because of the diversity and complexity of pollution sources, composite air pollution has become the main mode of pollution in many countries [7–9], and thus, its management is gaining increasing attention. Among pollutants, PM$_{2.5}$ and O$_3$ share the same precursors and usually exhibit strong spatial and temporal correlations [10–12]. Considering that each of these pollutants can influence the transformation of the other, composite pollution involving PM$_{2.5}$ and O$_3$ occurs in many regions worldwide [13–15]. This implies that high levels of both PM$_{2.5}$ and O$_3$ have been reported concurrently in many areas [16–19]. Therefore, PM$_{2.5}$ and O$_3$ are pollutants that are currently deteriorating ambient air quality in different areas globally.

In recent years, studies on PM$_{2.5}$ and O$_3$ pollution have focused on spatial and temporal characteristics, meteorological causes, and sources. According to these studies, PM$_{2.5}$ pollution is prevalent in winter, whereas O$_3$ pollution is dominant in summer [20–22], and

thus, $PM_{2.5}$–O_3 pollution exhibits apparent seasonal variations [23–26]. In areas such as the Yangtze River Delta, Pearl River Delta, Fenwei Plain, and Beijing–Tianjin–Hebei region, $PM_{2.5}$–O_3 pollution has been increasing in recent years [27–29]. $PM_{2.5}$ and O_3 share the same precursors—NOx and VOCs [30–32]—but interact in the atmosphere through diverse sources [33–35]. As the concentration of O_3 increases, oxidation in the atmosphere also gradually increases [36–39], whereas photolysis of NO_2 that generates OH radicals reduces the concentration of NO_2 and inhibits the production of $PM_{2.5}$ [31,37,40]. Conversely, an increase in the concentration of $PM_{2.5}$ weakens solar radiation and reduces the occurrence of photoreactions, thereby reducing the concentration of O_3 [41–43]. Meteorological factors also influence $PM_{2.5}$–O_3 pollution variably; high temperature and low humidity favor the generation of O_3, but these can inhibit the production of $PM_{2.5}$ [44–46]. According to back trajectory models, $PM_{2.5}$–O_3 pollution has been principally assigned to local and exogenous sources [17,47–49]. Existing studies on $PM_{2.5}$–O_3 pollution in areas such as the Yangtze River Delta, Pearl River Delta, Beijing–Tianjiny–Hebei region, and Fenwei Plain have focused on the short term, and thus, long-term studies for urban agglomerations such as the Central Plains are unavailable.

The Central Plains is a national strategic urban agglomeration in the middle reaches of the Yellow River Basin. It is an important hub through which the east and west and north and south are connected, and thus, its potential and advantages in relation to development are immense. Concerning the topography, the Central Plains Urban Agglomeration is dominantly flat, and its prominent inter-urban pollutant emission effects exacerbate the pollution levels in different areas [50–52]. The key cities in the Central Plains urban agglomeration (Anyang, Hebi, Puyang, Xinxiang, Kaifeng, Zhengzhou, and Jiaozuo), which are in the Beijing–Tianjin–Hebei air pollution transmission corridor, are increasingly experiencing problems regarding air pollution. Therefore, in the present study, $PM_{2.5}$–O_3 concentrations and related meteorological data were utilized to assess the spatial and temporal characteristics, the controlling meteorological factors, and the potential sources of this composite pollutant to improve our understanding of its magnitude in the Central Plains Urban Agglomeration. The findings of this study are expected to provide a theoretical basis for the management of $PM_{2.5}$–O_3 pollution in major cities in the Central Plains and for the integrated prevention and control of pollution in the region.

2. Materials and Methods

2.1. Study Area and Meteorological Data

The $PM_{2.5}$ and O_3 data used in the present study were obtained from the Environmental Protection Bureau of cities in Henan Province. The meteorology data (temperature, relative humidity, wind direction, and wind speed) were retrieved from hourly recordings of meteorological stations that are available in the Henan Meteorological and Environmental Center, and the distribution of these stations are shown in Figure 1. Data covering the period from 1 January 2014 to 31 December 2020 for Puyang, Hebi, Anyang, Jiaozuo, Xinxiang, Kaifeng, and Zhengzhou in the Central Plains were utilized in the present study.

According to the Ambient Air Quality Standard (GB3095-2012) and secondary standards of the concentration limits of pollutants in the National Air Quality Standards, a daily average $\rho(PM_{2.5}) > 75\ \mu g/m^3$ and a daily maximum 8 h sliding average $\rho(O_3) > 160\ \mu g/m^3$ were used to define a $PM_{2.5}$–O_3 pollution day as one in which both pollutants exceeded the standard levels. Similarly, a day in which only $PM_{2.5}$ was higher than the National Secondary Standard value was termed a $PM_{2.5}$ pollution day, whereas that with just a higher O_3 concentration was referred to as an O_3 pollution day.

According to the meteorological industry standard of the China Meteorological Administration (QX/T152-2012), the months associated with different seasons are the following: March–May for spring, June–August for summer, September–November for autumn, and December–February for winter. The back trajectory analysis was conducted using the 2014–2020 Global Data Assimilation System (GDAS) data that were obtained from the U.S. National Centers for Environmental Prediction (NCEP).
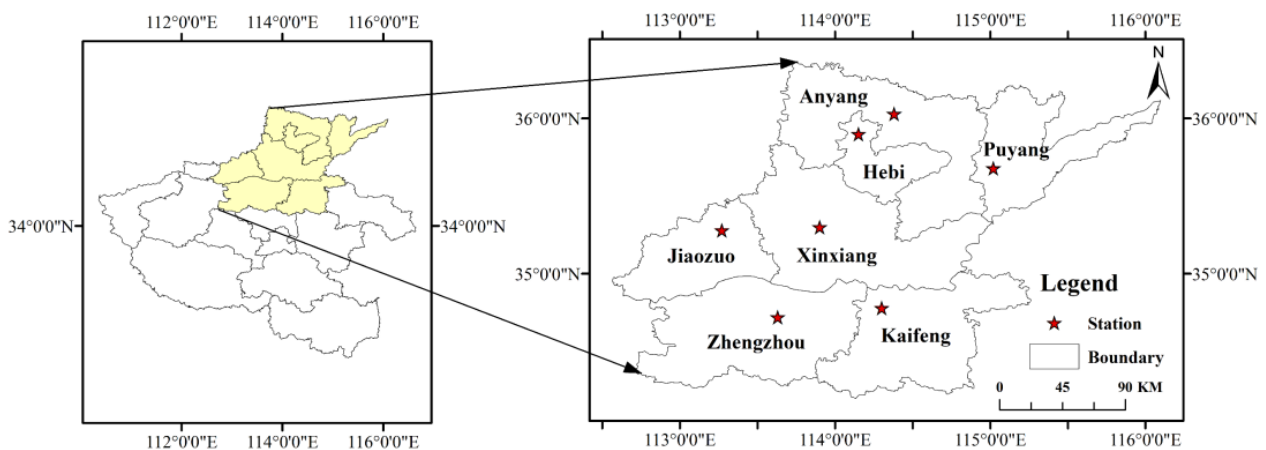
Figure 1. Overview of the study area. The stations in the figure (red stars) indicate conventional ground-based meteorological stations in major cities in the Central Plains Urban Agglomeration.

2.2. Back Trajectory Analysis and Trajectory Clustering

In the present study, the posterior trajectory clustering involving a potential source contribution function (PSCF) model was utilized to determine transport pathways and potential source areas of pollutants in the study area through an integration of measured chemical concentrations and recorded meteorological data. The posterior trajectory clustering and PSCF analysis were conducted using the TrajStat plugin in the MeteoInfo 3.3.0 open source software developed by the Chinese Academy of Meteorological Sciences (Java Edition). Xinxiang (35.30° N and 113.92° E), which displayed the highest number of $PM_{2.5}$–O_3 pollution days (see the "Results and Discussion" section for further details), was considered a receiving point, whereas the starting height was set to 500 m (a height of 500 m can reflect the characteristics of the average atmospheric flow field), and these parameters were utilized to simulate 24 h back trajectories for different seasons from 1 January 2014 to 31 December 2020 (12:00 UTC), in association with GDAS flow field data. A systematic clustering method was used to group trajectories that reached the receiving point. All trajectories were regarded as different n classes, and the closest two were initially combined into a class, followed by others, until an optimum result was obtained.

2.3. Analysis of Potential Sources

In the PSCF model, air mass trajectories passing through a region are considered influenced by local emissions, and thus, this contributes to concentrations of pollutants at an observation point associated with transport. The PSCF value was obtained from segmented endpoints of a trajectory under the spatial resolution of the grid using the following expression:

$$PSCF = \frac{m_{i,j}}{n_{i,j}} \tag{1}$$

where $n_{i,j}$ is the number of endpoints of a trajectory of the (i, j) grid, and $m_{i,j}$ is the number of endpoints of the trajectory of the (i, j) grid that exceed the threshold. The thresholds were set according to the Ambient Air Quality Standard (GB3095-2012) and the concentration limits of pollutants in the National Air Quality Standards to a daily average of >75 μg/m^3 for $PM_{2.5}$ and a daily maximum 8 h sliding average (O_3–8 h) of >160 μg/m^3 for O_3. When $n_{i,j}$ is small, the results of PSCF will be large and have a large uncertainty range. In order to reduce this uncertainty, a weight function W_{ij} (Equation (2)) was introduced in the present study. When $n_{i,j}$ in a grid is less than three times the average number of trajectory endpoints per grid (n_{ave}), W_{ij} is needed to reduce the uncertainty of the PSCF results [53].

The Weighted PSCF model (WPSCF) derived from the addition of weights improves the location of potential source regions [54,55].

$$W_{ij} = \begin{cases} 1.00 & 3n_{ave} < n_{i,j} \\ 0.70 & 1.5n_{ave} < n_{i,j} \leq 3n_{ave} \\ 0.40 & n_{ave} \leq n_{i,j} \leq 1.5n_{ave} \\ 0.17 & n_{i,j} \leq n_{ave} \end{cases} \tag{2}$$

3. Results and Discussion

3.1. Spatial and Temporal Characteristics of $PM_{2.5}$–O_3 Pollution

3.1.1. Spatial Characteristics of $PM_{2.5}$–O_3 Pollution

As shown in Figure 2, the $PM_{2.5}$–O_3 pollution days for cities in the Central Plains Urban Agglomeration were clustered around Xinxiang, and these days decreased toward the north and south. The $PM_{2.5}$–O_3 pollution days in spring exhibited the highest values throughout the study area and followed an expansive trend from the center to the northeast and southwest. Xinxiang showed the highest number of compound pollution days (31 days), whereas Hebi had the lowest number (8 days). Conversely, in the summer, $PM_{2.5}$–O_3 compounded pollution days were concentrated in the northwest of the study area, and the highest occurrences of 36 and 33 days were in Jiaozuo and Xinxiang, respectively. Hebi also showed the lowest number of compound pollution days (6 days) in the study area. In autumn, the $PM_{2.5}$–O_3 compound pollution days were highest in the northwest of the study area, and Zhengzhou and Xinxiang displayed the highest number of pollution days (12 and 11, respectively), whereas other regions had less than 10 days. Finally, in winter, no $PM_{2.5}$–O_3 pollution days occurred in the entire region.
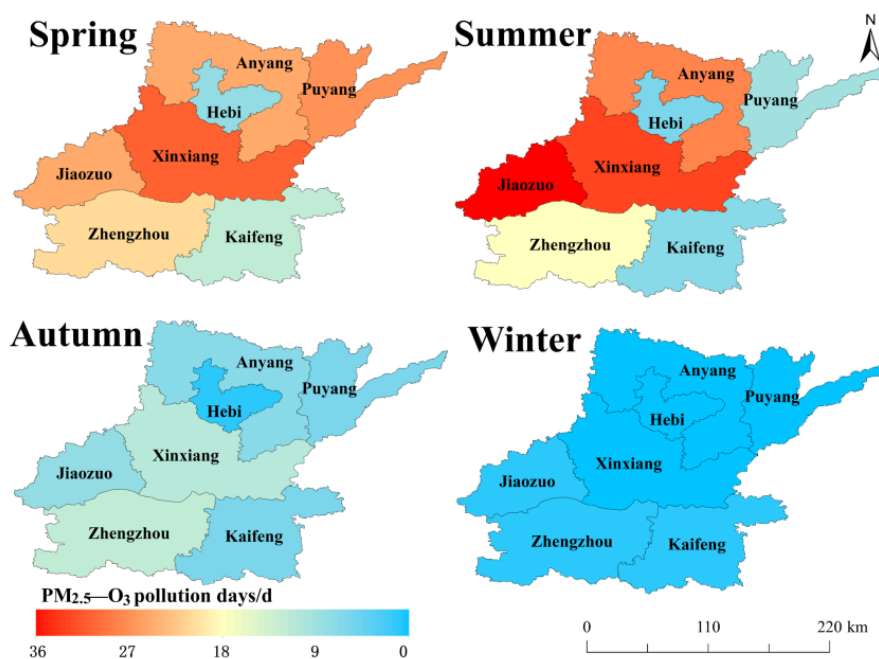

Figure 2. Plots showing the seasonal variations of $PM_{2.5}$–O_3 pollution days in the key cities of the Central Plains Urban Agglomeration from 2014 to 2020.

As shown in Figure 2, the number of compound pollution days in Hebi was lower than in the surrounding areas in all seasons. This was likely due to the topography around Hebi, as it is located between Anyang, Puyang, and Hebi, and thus the pollutants are blocked by the mountains and cannot easily spread to Hebi.

3.1.2. Temporal Characteristics of PM$_{2.5}$–O$_3$ Pollution

As shown in Figure 3a, during the period from 2014 to 2020, 50 days of PM$_{2.5}$–O$_3$ pollution occurred in the cities of the Central Plains Urban Agglomeration that were studied. Overall, this pollution decreased from 15 days in 2014 to 1 day in 2020. The ρ(PM$_{2.5}$) data exhibited an M-like shape, and the highest value of 108 μg/m^3 occurred in 2019, whereas the lowest value of 70 μg/m^3 emerged in 2017. The second highest value of 102 μg/m^3 was found for 2014 and decreased to 70 μg/m^3 in 2017. However, ρ(PM$_{2.5}$) then increased to 78 and 108 μg/m^3 in 2018 and 2019, respectively, whereas the ρ(O$_3$) data exhibited a V-like shape, and the highest and lowest values of 210 and 152 μg/m^3 were correspondingly associated with 2020 and 2018, respectively. As shown in Figure 3b, according to the monthly distribution, the PM$_{2.5}$–O$_3$ pollution days were concentrated in the spring and summer of each year (April–July). The month of June showed the maximum monthly occurrence of 13 days, followed by May with 11 days, whereas the late autumn and winter months (November–February) had no PM$_{2.5}$–O$_3$ pollution days. Variations in the meteorological conditions during different seasons may cause significant differences in the generation and propagation of PM$_{2.5}$–O$_3$ pollution [8,11,32], and this may account for the seasonal differences observed in the present study.
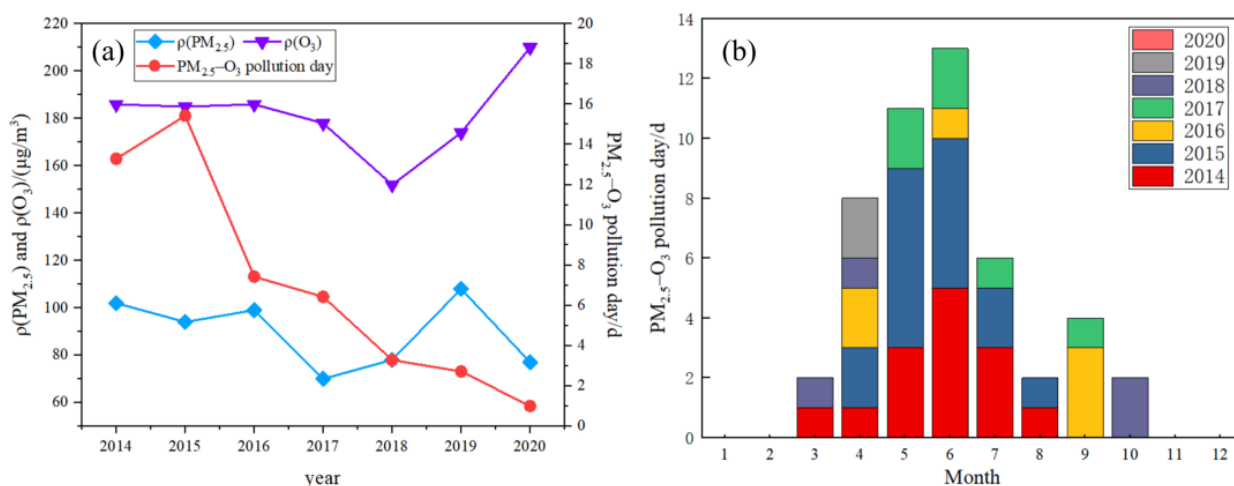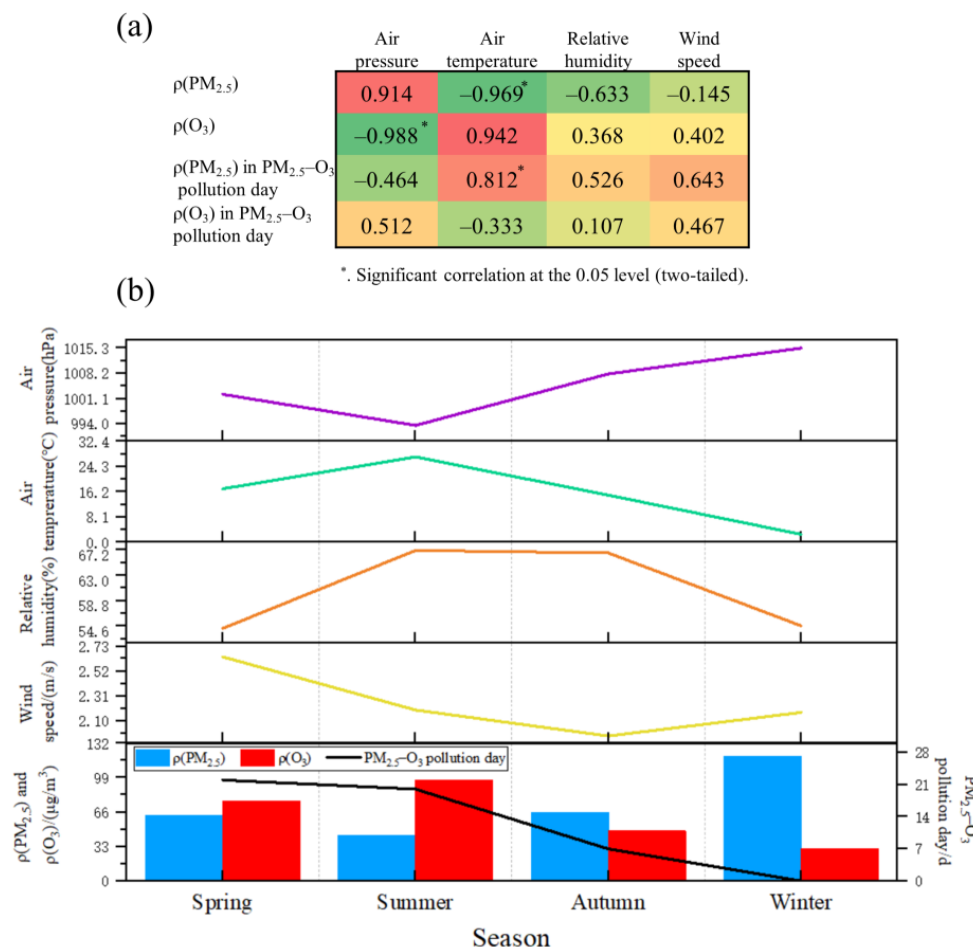

Figure 3. (**a**) Chart showing the Interannual distribution of PM$_{2.5}$, O$_3$ and PM$_{2.5}$–O$_3$ composite pollution days and (**b**) the intermonthly distribution of PM$_{2.5}$–O$_3$ composite pollution days.

3.2. Relationships between PM$_{2.5}$–O$_3$ Pollution and Meteorological Factors

Both PM$_{2.5}$ and O$_3$ are easily transported in the atmosphere, and, considering that these are products of complex photochemical reactions, their concentrations are strongly influenced by meteorological factors [29]. Therefore, the relationships between PM$_{2.5}$–O$_3$ pollution and meteorological factors were evaluated subsequently.

Figure 4a shows that the single pollutant and PM$_{2.5}$–O$_3$ pollution had a very complex relationship with air pressure and temperature. In fact, ρ(PM$_{2.5}$) exhibited a significant negative correlation with temperature (-0.969), and ρ(O$_3$) showed a strong negative correlation with air pressure (-0.988). However, ρ(PM$_{2.5}$) in PM$_{2.5}$–O$_3$ pollution days showed a significant positive correlation with temperature (0.812), and ρ(O$_3$) in PM$_{2.5}$–O$_3$ pollution days showed a significant positive correlation with air pressure (0.512). Figure 4a,b show that PM$_{2.5}$–O$_3$ pollution days occurred predominant in spring and summer, during which high temperatures and low pressures are common. The highest temperature in summer was 27.44 °C, whereas the lowest pressure was 993.56 hPa, and these conditions were associated with the lowest ρ(PM$_{2.5}$) of 44 μg/m^3 and the highest ρ(O$_3$) of 96.92 μg/m^3. In the winter, during which there were no days of PM$_{2.5}$–O$_3$ pollution, the lowest ρ(O$_3$) of 31.05 μg/m^3 and the highest ρ(PM$_{2.5}$) of 119.05 μg/m^3 were obtained. This season produced the minimum temperature of 2.55 °C and the maximum pressure 1015.30 hPa.

These results indicate that the absence of $PM_{2.5}$–O_3 pollution days in winter was mainly because a low–temperature and high–pressure environment is unsuitable for the generation of O_3, which reduced the occurrence of $PM_{2.5}$–O_3 pollution days.

(a)

	Air pressure	Air temperature	Relative humidity	Wind speed
$\rho(PM_{2.5})$	0.914	−0.969*	−0.633	−0.145
$\rho(O_3)$	−0.988*	0.942	0.368	0.402
$\rho(PM_{2.5})$ in $PM_{2.5}$–O_3 pollution day	−0.464	0.812*	0.526	0.643
$\rho(O_3)$ in $PM_{2.5}$–O_3 pollution day	0.512	−0.333	0.107	0.467

*. Significant correlation at the 0.05 level (two-tailed).

(b)

Figure 4. (**a**) Chart showing the correlations between $PM_{2.5}$–O_3 pollution and meteorological factors and (**b**) the seasonal variation of $PM_{2.5}$, O_3, and $PM_{2.5}$–O_3 pollution versus meteorological factors in the Central Plains Urban Agglomeration from 2014 to 2020. Note: the colors in (**a**) represent the degree of correlation, with red representing a positive correlation, yellow representing no correlation, and green representing a negative correlation.

The relative humidity values in summer (67.12%) and autumn (66.69%) were higher than those in spring (54.25%) and winter (54.67%). The proportion of $\rho(PM_{2.5})$ and $\rho(O_3)$ was not strongly influenced by changes in humidity, and this was probably due to the superposition of various factors such as temperature and wind speed, as well as the atmospheric content of ·OH, i.e., this might be due the production and accumulation of $PM_{2.5}$ and O_3 being influenced by multiple factors [42]. Therefore, the relationship between $PM_{2.5}$–O_3 pollution and relative humidity is complex.

Winds can promote the formation and dispersion of atmospheric pollutants, and thus, the relationships between wind speed and frequency and $PM_{2.5}$–O_3 pollution were also examined. Figure 4b shows that the maximum wind speed of 2.64 m/s occurred in spring, followed by 2.19 m/s in summer, whereas the minimum wind speed of 1.97 m/s was recorded in autumn. Regarding the wind direction frequency, Figure 5 shows that southerly winds prevailed in the spring and summer, whereas northerly winds were dominant in autumn and winter in the cities in the Central Plains Urban Agglomeration. Considering the seasonal differences in $PM_{2.5}$–O_3 pollution days and the frequency of this pollution in spring and summer, it is evident that as part of the Beijing–Tianjin–Hebei pollution

transmission channel cities, $PM_{2.5}$–O_3 pollution and O_3 precursors were promoted in the cities in the Central Plains Urban Agglomeration in the presence of southerly winds with speeds of 2.14–2.19 m/s. The increase of the $PM_{2.5}$–O_3 pollutant and O_3 precursors in the spring and summer was consistent with the predominantly southerly winds. The influence of wind direction and speed on pollutants in spring and summer involved two segments [4,24]. First, the $PM_{2.5}$–O_3 composite pollutant and O_3 precursors were transported to the study area by wind, which favored their generation and accumulation and, thus, the increase in their concentrations. Second, the winds in the study area also transported the $PM_{2.5}$–O_3 pollutant and O_3 precursors that were present in other areas, thereby causing daily variations in $PM_{2.5}$–O_3 pollution.
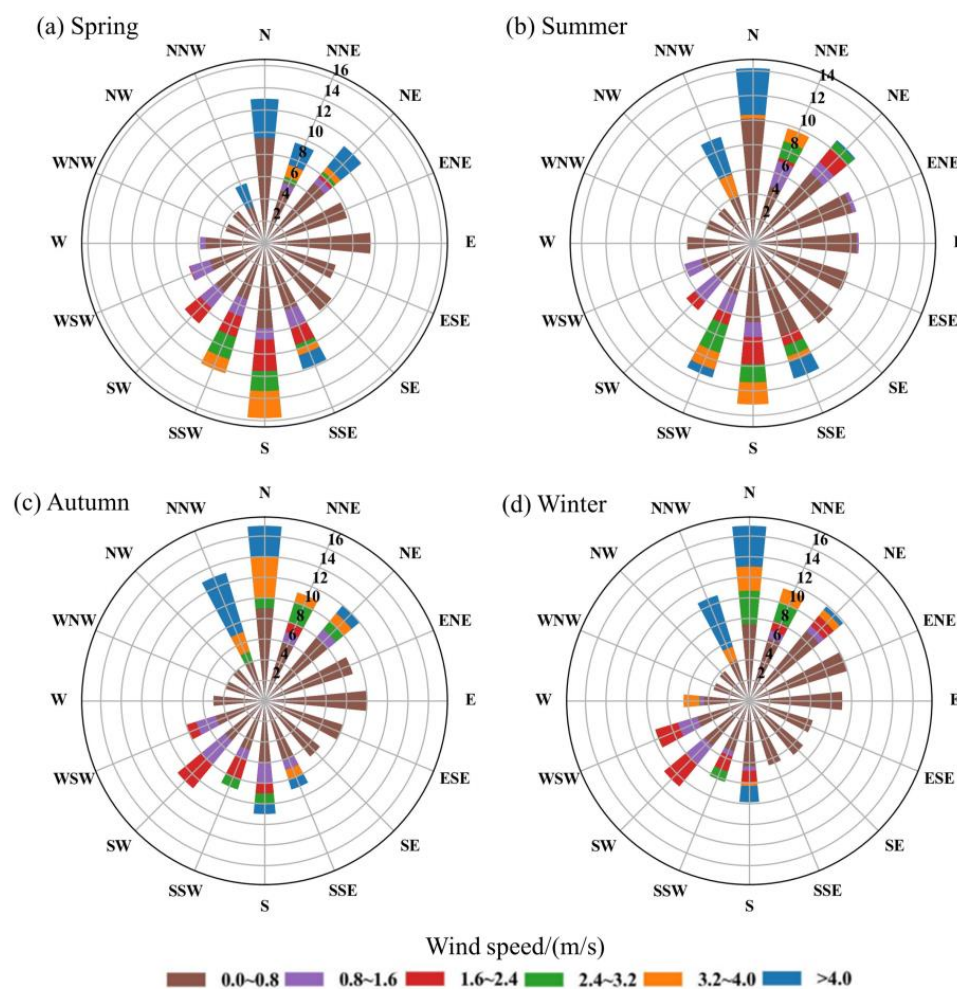
Figure 5. Plot showing the seasonal frequency distribution of wind speeds and directions associated with $PM_{2.5}$–O_3 pollution in the Central Plains Urban Agglomeration from 2014 to 2020. Note: the values inside the circles represent the cumulative frequency of wind speed in that direction (%). (**a**–**d**) represent spring, summer, autumn, winter.

3.3. Analysis of the $PM_{2.5}$–O_3 Pollution Sources

According to the back trajectory analysis of seasonal data, the air mass transport paths varied significantly, and the external transport ranges of the pollutants were high. Based on the inflection point of the total spatial variance of the trajectory clustering, the inputs of $\rho(PM_{2.5})$ and $\rho(O_3)$ could be grouped into six major airflow trajectories for all seasons, and these are presented in Table 1.

Table 1. Clustering data of the posterior term trajectories in different seasons.

Season	No.	Frequency of Occurrence(%)	Route Area	$\rho(O_3)$ $(\mu g/m^3)$	$\rho(PM_{2.5})$ $(\mu g/m^3)$
Spring	1	26.09	Puyang	95.1	55.6
	2	8.70	Northeastern Inner Mongolia, Hebei Province, Beijing	101.3	35.3
	3	15.22	Southwestern Inner Mongolia, Northern Shaanxi Province, Southern Shaanxi Province	99.0	39.6
	4	23.91	Southern Henan Province	120.2	51.1
	5	16.30	Southern Shanxi Province	113.0	53.4
	6	9.78	Bohai	71.3	39.2
Summer	1	14.13	Southern Henan Province	130.8	21.6
	2	28.26	Northwestern Jiangsu Province, southwestern Shandong Province	118.4	30.6
	3	9.78	Northern Shandong Province, Southern Hebei Province	102.2	22.7
	4	16.30	Southwestern Hebei Province	119.1	31.8
	5	26.09	Central Henan Province	174.9	28.9
	6	5.43	Southern Inner Mongolia, western Hebei Province, south	126.7	22.8
Autumn	1	16.48	Southern Hebei Province	48.2	57.2
	2	20.88	Southern Shanxi Province	64.3	97.6
	3	3.30	Western Inner Mongolia, Southern, Northern Shaanxi Province, Southern Shaanxi Province	54.6	55.5
	4	35.16	Eastern Henan Province	38.4	91.2
	5	8.79	Northern Shaanxi Province, Southern Shaanxi Province	63.0	24.8
	6	15.38	Eastern Hebei Province, northwestern Bohai Sea, northwestern Shandong Province, southern Hebei Province	50.6	90.1
Winter	1	20.51	Southwestern Inner Mongolia, Northern Shaanxi Province, Southern Shaanxi Province	40.1	79.0
	2	2.56	Eastern Henan Province	30.8	90.8
	3	21.79	Southern Shanxi Province	30.3	113.7
	4	14.10	Northern Shanxi Province, Southern Hebei Province	32.6	63.6
	5	23.08	Central and Northern Henan Province	22.4	105.4
	6	17.95	Southern Hebei Province	28.6	97.4

In the study area, the air currents that were responsible for the input of pollutants in spring were mainly No. 1 from Puyang and No. 4 from the south of Henan. These currents, which accounted for 50% of the frequency, contributed 120.2 and 55.6 $\mu g/m^3$ of $\rho(PM_{2.5})$ and $\rho(O_3)$, respectively. In addition to the data shown in Figure 6a, the sources of $PM_{2.5}$ pollution in spring were mainly in the central part of Henan (south of Kaifeng, west of Zhoukou, and northeast of Zhumadian), and thus, pollution was minimally influenced by external factors. The WPSCF analysis for O_3 produced no evident range, but high values were found for Zhoukou and Fuyang.
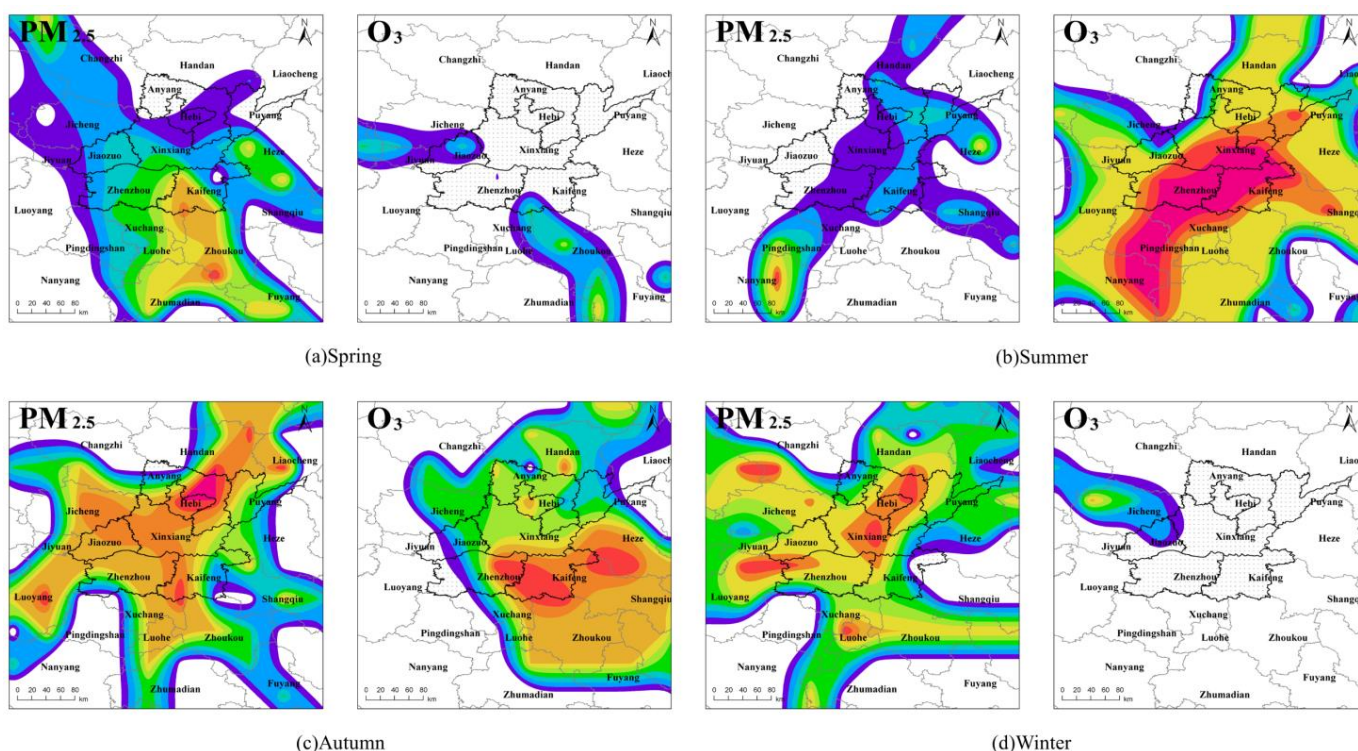
Figure 6. Characteristics of the WPSCF potential source contribution function distribution values of PM$_{2.5}$–O$_3$ compound pollution in the four seasons in key cities in the Central Plains Urban Agglomeration. Note: (**a**–**d**) represent spring, summer, autumn, winter.

Conversely, in summer, the dominant air currents were No. 2 from the northwest of Jiangsu Province and southwest of Lu and No. 5 from the central part of Yu, and these were associated with frequencies of 28.26% and 26.09%, respectively. For the pollutant input from the external air currents, the concentration of O$_3$ in summer was 2–3 times higher than in autumn and winter, while the input PM$_{2.5}$ was the lowest of the year. Owing to the favorable temperature and humidity, ρ(O$_3$) in summer was high, and its transmission intensity was enhanced. The results and data shown in Figure 6b revealed that potential sources of high PM$_{2.5}$ pollution were the northeastern part of Nanyang and the central part of Heze. Pollutants generated in the north of the Beijing–Tianjin–Hebei region are easily transported to the study area because of the prevailing wind direction, and this explained the prominent pollution trajectories. In contrast, the potential source areas of O$_3$ appeared predominantly in the central part of Henan Province (Xinxiang, Zhengzhou, Kaifeng, Xuchang, Pingdingshan, and Shangqiu) and in the west of Shandong Province (Heze). High values were also obtained from the WPSCF analysis, which demonstrated that most of O$_3$ pollution during the period that was studied originated within the study area.

Relatedly, in autumn, the principal air currents were No. 4 from the east of Yu and No. 2 from the south of Lu, and these represented frequencies of 35.16% and 20.88%, respectively, and the provincial sources exceeded 30%. The maximum inputs of 64.3 and 97.6 µg/m^3 corresponding to ρ(PM$_{2.5}$) and ρ(O$_3$), respectively, were both associated with the No. 2 air current from the south of Shanxi Province. Figure 6c shows that the potential sources of PM$_{2.5}$ were mainly in Henan Province (Hebi, central part of Anyang, southwest of Kaifeng, and Luoyang). Lower but significant values were also associated with areas outside the province including Handan and Liaocheng. The diffused spatial distribution of high pollution in the study area was attributed to the prevailing northerly winds in autumn. Potential source areas were in the south of the study area (Zhengzhou and Kaifeng) and southwest of Heze.

Lastly, in winter, the prevalent air currents were No. 5 from the center of Henan Province, No. 3 from the south of Shanxi Province, and No. 1 from different places in the northwest of the study area. The occurrence frequency of these air currents accounted for more than 20%. Hence, the the winter airflow mainly originated from the interior and northwest of Henan Province. The No. 1 current contributed the highest O_3 concentration of 40.1 μg/m^3, whereas No. 3 was responsible for the maximum $\rho(PM_{2.5})$ input of 113.7 μg/m^3. According to these results and data shown in Figure 6d, high $\rho(PM_{2.5})$ values during winter were recorded in the east of Anyang, Hebi, Xinxiang, and Luoyang. The wide range of airflow sources available in winter indicated that under low–temperature conditions, contaminating precursors travel farther and have greater impacts. Potential sources of $PM_{2.5}$ were dominantly found in the province, and these were related to the burning of fuels for heating during winter. Even though a significant potential source area of O_3 was not evident, Jincheng is an area from which high values were obtained.

In summary, in addition to the local emissions, $PM_{2.5}$–O_3 pollution appeared influenced by the transport of pollutants between neighboring cities. Changes in the seasons altered the transport pathways of the pollutants in and outside the study area. Potential source areas of the pollutants were not evident from winter to spring, but in summer and autumn, Heze, which is adjacent to Henan Province, appeared as a main potential source.

This paper has certain limitations. The effects of $PM_{2.5}$–O_3 pollution involve complex processes, which are also related to the production and transport of its precursors and the interactions of chemical substances. Therefore, further studies on $PM_{2.5}$–O_3 pollution need to be carried out by researchers.

4. Conclusions

Based on the pollutant data of $PM_{2.5}$ and O_3, as well as on meteorological data, this paper investigated the spatial and temporal characteristics of $PM_{2.5}$–O_3 pollution in key cities of the Central Plains Urban Agglomeration from 2014 to 2020, analyzed the effects of corresponding meteorological conditions on $PM_{2.5}$–O_3 pollution in each season, and explored the potential sources of the pollutants using backward trajectory and potential source analysis methods. The principal findings can be summarized as follows:

(a) Spatially, the $PM_{2.5}$–O_3 pollution days in the Central Plains Urban Agglomeration were clustered around the center of Xinxiang and then decreased toward the north and south. The highest concentration of $PM_{2.5}$–O_3 during the pollution days occurred in the spring for the entire study area, and the trend expanded from the center to the northeast and southwest. Temporally, during the period from 2014 to 2020, 50 days of $PM_{2.5}$–O_3 pollution occurred in major cities in the Central Plains Urban Agglomeration, with a maximum of 15 composite pollution days in 2015 and a minimum of 1 day in 2020, and the overall trend of the interannual variation of composite pollution in the major cities of the Central Plains urban agglomeration decreased in combination. According to the monthly distribution, the $PM_{2.5}$–O_3 pollution days were concentrated in the spring and summer of each year. The month of June was associated with the highest number of pollution days (13), followed by May (11), whereas no $PM_{2.5}$–O_3 pollution day was observed in the late autumn and winter (November–February).

(b) Regarding the influence of meteorological factors, composite, $\rho(PM_{2.5})$, and $\rho(O_3)$ pollution exhibited strong correlations with the air pressure and temperature. The parameter $\rho(PM_{2.5})$ was significantly negatively correlated with the air temperature (−0.969), whereas $\rho(O_3)$ was significantly negatively correlated with the air pressure (−0.988). The results associated with a temperature of 2.55 °C and an air pressure of 1015.30 hPa revealed that a low–temperature and high–pressure environment was not conducive to the generation of a $PM_{2.5}$–O_3 pollution day. As part of the Beijing–Tianjin–Hebei pollution transmission corridor, the major cities in the Central Plains Urban Agglomeration appeared as favorable areas for the accumulation of the $PM_{2.5}$–O_3 pollutant and O_3 precursors when the wind speed varied from 2.14 to

2.19 m/s, and the winds were southerly. These conditions promoted the occurrence of $PM_{2.5}$–O_3 pollution days.

(c) The transport paths of air masses varied significantly among the seasons, and the external contributions of pollutants in spring, autumn, and winter were higher than in summer. The inflow of $PM_{2.5}$–O_3 pollution in spring originated mainly from provinces around the study area. The input of $\rho(O_3)$ was highest from the central part of Henan Province in summer, whereas that of $\rho(PM_{2.5})$ was predominantly from the southwest of Hebei Province. In autumn, inputs of both $\rho(PM_{2.5})$ and $\rho(O_3)$ originated mainly from the south of Shanxi Province, whereas in winter, $\rho(O_3)$ was transported from many areas in the northwest of the study area, but the highest input of $\rho(PM_{2.5})$ was from the south of Shanxi Province. The potential sources of $PM_{2.5}$ were shifted and diffused by the prevailing winds from the central part of Henan Province in spring to the south (northeast of Nanyang and center of Heze) in summer. In autumn and winter, these sources were mainly in the study area, including the central part of Anyang, Hebi, Xinxiang, Zhengzhou, and Kaifeng. Potential source areas for O_3 were not evident in spring and winter, whereas in summer and autumn, O_3 pollution originated mainly from areas in the province and from Heze city in Shandong province, which is adjacent to Henan Province.

This study revealed the spatial and temporal variation of $PM_{2.5}$–O_3 pollution in key cities of the Central Plains Urban Agglomeration in recent years and the seasonal meteorological characteristics affecting its concentration. Additionally, it showed the influence of seasonal regional transport. Due to the limited data on pollutants and the scope of the analysis methods, further research is needed to combine long–term fine meteorological and environmental observations with the analysis of chemical reactions between pollutants. This will improve our understanding of $PM_{2.5}$–O_3 pollution.

Conflicts of Interest: The authors declare no conflict of interest.

References

1. Baker, K.R.; Woody, M.C. Assessing model characterization of single source secondary pollutant impacts using 2013 SENEX field study measurements. *Environ. Sci. Technol.* **2017**, *51*, 3833–3842. [CrossRef]
2. Alghamdi, M.A.; Shamy, M.; Ana Redal, M.; Khoder, M.; Awad, A.H.; Elserougy, S. Microorganisms associated particulate matter: A preliminary study. *Sci. Total Environ.* **2014**, *479*, 109–116. [CrossRef]
3. Tan, Y.; Wang, H.; Zhu, B.; Zhao, T.; Shi, S.; Liu, A.; Liu, D.; Pan, C.; Cao, L. The interaction between black carbon and planetary boundary layer in the Yangtze River Delta from 2015 to 2020: Why O_3 didn't decline so significantly as $PM_{2.5}$. *Environ. Res.* **2022**, *214*, 114095. [CrossRef]
4. Wang, L.; Li, M.; Wang, Q.; Li, Y.; Xin, J.; Tang, X.; Du, W.; Song, T.; Li, T.; Sun, Y.; et al. Air stagnation in China: Spatiotemporal variability and differing impact on $PM_{2.5}$ and O_3 during 2013–2018. *Sci. Total Environ.* **2022**, *819*, 152778. [CrossRef]

5. Li, L.; Mi, Y.; Lei, Y.; Wu, S.; Li, L.; Hua, E.; Yang, J. The spatial differences of the synergy between CO_2 and air pollutant emissions in China's 296 cities. *Sci. Total Environ.* **2022**, *846*, 157323. [CrossRef]

6. Liao, Z.; Gao, M.; Sun, J.; Fan, S. The impact of synoptic circulation on air quality and pollution–related human health in the Yangtze River Delta region. *Sci. Total Environ.* **2017**, *607*, 838–846. [CrossRef]

7. Lin, H.; Guo, Y.; Ruan, Z.; Yang, Y.; Chen, Y.; Zheng, Y.; Cummings–Vaughn, L.A.; Rigdon, S.E.; Vaughn, M.G.; Sun, S.; et al. Ambient $PM_{2.5}$ and O_3 and their combined effects on prevalence of presbyopia among the elderly: A cross–sectional study in six low– and middle–income countries. *Sci. Total Environ.* **2019**, *655*, 168–173. [CrossRef]

8. Wang, P.; Guo, H.; Hu, J.; Kota, S.H.; Ying, Q.; Zhang, H. Responses of $PM_{2.5}$ and O_3 concentrations to changes of meteorology and emissions in China. *Sci. Total Environ.* **2019**, *662*, 297–306. [CrossRef]

9. Wu, Z.; Zhang, Y.; Zhang, L.; Huang, M.; Zhong, L.; Chen, D.; Wang, X. Trends of outdoor air pollution and the impact on premature mortality in the Pearl River Delta region of southern China during 2006–2015. *Sci. Total Environ.* **2019**, *690*, 248–260. [CrossRef]

10. Liu, G.-J.; Su, F.-C.; XU, Q.-X.; Zhang, R.-Q.; Wang, K. One–year simulation of air pollution in central China, characteristics, distribution, inner region cross–transmission, and pathway research in 18 cities. *Huan Jing Ke Xue Huanjing Kexue* **2022**, *43*, 3953–3965. [CrossRef]

11. Xiao, Z.-M.; Li, Y.; Kong, J.; Li, P.; Cai, Z.-Y.; Gao, J.-Y.; Xu, H.; Ji, Y.-F.; Deng, X.-W. Characteristics and meteorological factors of $PM_{2.5}$–O_3 compound pollution in Tianjin. *Huan Jing Ke Xue Huanjing Kexue* **2022**, *43*, 2928–2936. [CrossRef] [PubMed]

12. Malakootian, M.; Mohammadi, A. Estimating health impact of exposure to $PM_{2.5}$, No_2 and O_3 using AirQ plus model in Kerman, Iran. *Environ. Eng. Manag. J.* **2020**, *19*, 1317–1323.

13. Kazemiparkouhi, F.; Eum, K.-D.; Wang, B.; Manjourides, J.; Suh, H.H. Long–term ozone exposures and cause–specific mortality in a US medicare cohort. *J. Expo. Sci. Environ. Epidemiol.* **2020**, *30*, 650–658. [CrossRef] [PubMed]

14. Mekonnen, Z.K.; Oehlert, J.W.; Eskenazi, B.; Shaw, G.M.; Balmes, J.R.; Padula, A.M. The relationship between air pollutants and maternal socioeconomic factors on preterm birth in California urban counties. *J. Expo. Sci. Environ. Epidemiol.* **2021**, *31*, 503–513. [CrossRef] [PubMed]

15. Lee, H.K.; Choi, E.L.; Lee, H.J.; Lee, S.Y.; Lee, J.Y. A Study on the seasonal correlation between O_3 and $PM_{2.5}$ in Seoul in 2017. *J. Korean Soc. Atmos. Environ.* **2020**, *36*, 533–542. [CrossRef]

16. Faridi, S.; Shamsipour, M.; Krzyzanowski, M.; Kunzli, N.; Amini, H.; Azimi, F.; Malkawi, M.; Momeniha, F.; Gholampour, A.; Hassanvand, M.S.; et al. Long–term trends and health impact of $PM_{2.5}$ and O_3 in Tehran, Iran, 2006–2015. *Environ. Int.* **2018**, *114*, 37–49. [CrossRef]

17. Gao, A.; Wang, J.; Luo, J.; Wang, P.; Chen, K.; Wang, Y.; Li, J.; Hu, J.; Kota, S.H.; Zhang, H. Health and economic losses attributable to $PM_{2.5}$ and ozone exposure in Handan, China. *Air Qual. Atmos. Health* **2021**, *14*, 605–615. [CrossRef]

18. Wang, Y.; Hu, J.; Huang, L.; Li, T.; Yue, X.; Xie, X.; Liao, H.; Chen, K.; Wang, M. Projecting future health burden associated with exposure to ambient $PM_{2.5}$ and ozone in China under different climate scenarios. *Environ. Int.* **2022**, *169*, 107542. [CrossRef]

19. Zhang, H.; Zhu, A.; Liu, L.; Zeng, Y.; Liu, R.; Ma, Z.; Liu, M.; Bi, J.; Ji, J.S. Assessing the effects of ultraviolet radiation, residential greenness and air pollution on vitamin D levels: A longitudinal cohort study in China. *Environ. Int.* **2022**, *169*, 107523. [CrossRef]

20. He, C.; Hong, S.; Zhang, L.; Mu, H.; Xin, A.; Zhou, Y.; Liu, J.; Liu, N.; Su, Y.; Tian, Y.; et al. Global, continental, and national variation in $PM_{2.5}$, O_3, and NO_2 concentrations during the early 2020 COVID-19 lockdown. *Atmos. Pollut. Res.* **2021**, *12*, 136–145. [CrossRef]

21. Gao, L.; Yue, X.; Meng, X.; Du, L.; Lei, Y.; Tian, C.; Qiu, L. Comparison of ozone and $PM_{2.5}$ concentrations over urban, suburban, and background sites in China. *Adv. Atmos. Sci.* **2020**, *37*, 1297–1309. [CrossRef]

22. Reames, T.G.; Bravo, M.A. People, place and pollution: Investigating relationships between air quality perceptions, health concerns, exposure, and individual– and area–level characteristics. *Environ. Int.* **2019**, *122*, 244–255. [CrossRef]

23. Lamichhane, D.K.; Jung, D.-Y.; Shin, Y.-J.; Lee, K.-S.; Lee, S.-Y.; Ahn, K.; Kim, K.W.; Shin, Y.H.; Suh, D.I.; Hong, S.-J.; et al. Association of ambient air pollution with depressive and anxiety symptoms in pregnant women: A prospective cohort study. *Int. J. Hyg. Environ. Health* **2021**, *237*, 113823. [CrossRef]

24. Lili, W.; Yuesi, W.; Dongsheng, J.I.; Jinyuan, X.I.N.; Bo, H.U.; Wanjun, W. Characteristics of atmospheric pollutants in Tianjin Binhai new area during autumn and winter. *China Environ. Sci.* **2011**, *31*, 1077–1086.

25. Chen, Q.; Chen, Q.; Wang, Q.; Xu, R.; Liu, T.; Liu, Y.; Ding, Z.; Sun, H. Particulate matter and ozone might trigger deaths from chronic ischemic heart disease. *Ecotoxicol. Environ. Saf.* **2022**, *242*, 113931. [CrossRef]

26. Chang, L.-T.; Hong, G.-B.; Weng, S.-P.; Chuangd, H.-C.; Chang, T.-Y.; Liu, C.-W.; Chuang, W.-Y.; Chuang, K.-J. Indoor ozone levels, houseplants and peak expiratory flow rates among healthy adults in Taipei, Taiwan. *Environ. Int.* **2019**, *122*, 231–236. [CrossRef]

27. Lin, G.-Y.; Chen, H.-W.; Chen, B.J.; Chen, S.-C. A machine learning model for predicting $PM_{2.5}$ and nitrate concentrations based on long–term water–soluble inorganic salts datasets at a road site station. *Chemosphere* **2022**, *289*, 133123. [CrossRef]

28. Wang, L.; Xing, L.; Wu, X.; Sun, J.; Kong, M. Spatiotemporal variations and risk assessment of ambient air O_3, PM_{10} and $PM_{2.5}$ in a coastal city of China. *Ecotoxicology* **2021**, *30*, 1333–1342. [CrossRef]

29. Luo, Y.; Zhao, T.; Yang, Y.; Zong, L.; Kumar, K.R.; Wang, H.; Meng, K.; Zhang, L.; Lu, S.; Xin, Y. Seasonal changes in the recent decline of combined high $PM_{2.5}$ and O_3 pollution and associated chemical and meteorological drivers in the Beijing–Tianjin–Hebei region, China. *Sci. Total Environ.* **2022**, *838*, 156312. [CrossRef]

30. Wu, B.; Liu, C.; Zhang, J.; Du, J.; Shi, K. The multifractal evaluation of PM$_{2.5}$–O$_3$ coordinated control capability in China. *Ecol. Indic.* **2021**, *129*, 107877. [CrossRef]

31. Zhang, X.; Cheng, C.; Zhao, H. A health impact and economic loss assessment of O$_3$ and PM$_{2.5}$ exposure in Chino from 2015 to 2020. *Geohealth* **2022**, *6*, e2021GH000531. [CrossRef] [PubMed]

32. He, Z.; Liu, P.; Zhao, X.; He, X.; Liu, J.; Mu, Y. Responses of surface O$_3$ and PM$_{2.5}$ trends to changes of anthropogenic emissions in summer over Beijing during 2014–2019: A study based on multiple linear regression and WRF–Chem. *Sci. Total Environ.* **2022**, *807*, 150792. [CrossRef]

33. Zhu, J.; Chen, L.; Liao, H.; Yang, H.; Yang, Y.; Yue, X. Enhanced PM$_{2.5}$ decreases and O$_3$ increases in China during COVID-19 lockdown by aerosol–radiation feedback. *Geophys. Res. Lett.* **2021**, *48*, e2020GL090260. [CrossRef]

34. Sui, X.; Zhang, J.; Zhang, Q.; Sun, S.; Lei, R.; Zhang, C.; Cheng, H.; Ding, L.; Ding, R.; Xiao, C.; et al. The short–term effect of PM$_{2.5}$/O$_3$ on daily mortality from 2013 to 2018 in Hefei, China. *Environ. Geochem. Health* **2021**, *43*, 153–169. [CrossRef] [PubMed]

35. Lei, R.; Zhu, F.; Cheng, H.; Liu, J.; Shen, C.; Zhang, C.; Xu, Y.; Xiao, C.; Li, X.; Zhang, J.; et al. Short–term effect of PM$_{2.5}$/O$_3$ on non–accidental and respiratory deaths in highly polluted area of China. *Atmos. Pollut. Res.* **2019**, *10*, 1412–1419. [CrossRef]

36. Wang, Q.; Wang, X.; Huang, R.; Wu, J.; Xiao, Y.; Hu, M.; Fu, Q.; Duan, Y.; Chen, J. Regional transport of PM$_{2.5}$ and O$_3$ based on complex network method and chemical transport model in the Yangtze River Delta, China. *J. Geophys. Res.–Atmos.* **2022**, *127*, e2021JD034807. [CrossRef]

37. Zhu, R.-G.; Xiao, H.-Y.; Wen, Z.; Zhu, Y.; Fang, X.; Pan, Y.; Chen, Z.; Xiao, H. Oxidation of proteinaceous matter by ozone and nitrogen dioxide in PM$_{2.5}$: Reaction mechanisms and atmospheric implications. *J. Geophys. Res.–Atmos.* **2021**, *126*, e2021JD034741. [CrossRef]

38. McClure, C.D.; Jaffe, D.A. Investigation of high ozone events due to wildfire smoke in an urban area. *Atmos. Environ.* **2018**, *194*, 146–157. [CrossRef]

39. Chang, Y.; Du, T.; Song, X.; Wang, W.; Tian, P.; Guan, X.; Zhang, N.; Wang, M.; Guo, Y.; Shi, J.; et al. Changes in physical and chemical properties of urban atmospheric aerosols and ozone during the COVID-19 lockdown in a semi–arid region. *Atmos. Environ. (Oxf. Engl. 1994)* **2022**, *287*, 119270. [CrossRef]

40. Zhang, Y.; West, J.J.; Mathur, R.; Xing, J.; Hogrefe, C.; Roselle, S.J.; Bash, J.O.; Pleim, J.E.; Gan, C.-M.; Wong, D.-C. Long–term trends in the ambient PM$_{2.5}$– and O$_3$–related mortality burdens in the United States under emission reductions from 1990 to 2010. *Atmos. Chem. Phys.* **2018**, *18*, 15003–15016. [CrossRef]

41. Che, W.; Li, A.T.Y.; Frey, H.C.; Tang, K.T.J.; Sun, L.; Wei, P.; Hossain, M.S.; Hohenberger, T.L.; Leung, K.W.; Lau, A.K.H. Factors affecting variability in gaseous and particle microenvironmental air pollutant concentrations in Hong Kong primary and secondary schools. *Indoor Air* **2021**, *31*, 170–187. [CrossRef]

42. Cifuentes, F.; Galvez, A.; Gonzalez, C.M.; Orozco–Alzate, M.; Aristizabal, B.H. Hourly ozone and PM$_{2.5}$ prediction using meteorological data–alternatives for cities with limited pollutant information. *Aerosol Air Qual. Res.* **2021**, *21*, 200471. [CrossRef]

43. Xing, J.; Ding, D.; Wang, S.; Dong, Z.; Kelly, J.T.; Jang, C.; Zhu, Y.; Hao, J. Development and application of observable response indicators for design of an effective ozone and fine–particle pollution control strategy in China. *Atmos. Chem. Phys.* **2019**, *19*, 13627–13646. [CrossRef]

44. Feng, T.; Zhao, S.; Bei, N.; Liu, S.; Li, G. Increasing atmospheric oxidizing capacity weakens emission mitigation effort in Beijing during autumn haze events. *Chemosphere* **2021**, *281*, 130855. [CrossRef]

45. Filonchyk, M.; Yan, H.; Li, X. Temporal and spatial variation of particulate matter and its correlation with other criteria of air pollutants in Lanzhou, China, in spring–summer periods. *Atmos. Pollut. Res.* **2018**, *9*, 1100–1110. [CrossRef]

46. Bravo, M.A.; Warren, J.L.; Leong, M.C.; Deziel, N.C.; Kimbro, R.T.; Bell, M.L.; Miranda, M.L. Where is air quality improving, and who benefits? A study of PM$_{2.5}$ and ozone over 15 years. *Am. J. Epidemiol.* **2022**, *191*, 1258–1269. [CrossRef]

47. Guerette, E.; Chang, L.T.–C.; Cope, M.E.; Duc, H.N.; Emmerson, K.M.; Monk, K.; Rayner, P.J.; Scorgie, Y.; Silver, J.D.; Simmons, J.; et al. Evaluation of regional air quality models over Sydney, Australia: Part 2, comparison of PM$_{2.5}$ and Ozone. *Atmosphere* **2020**, *11*, 233. [CrossRef]

48. Han, X.; Su, J.; Hong, Y.; Lai, P.; Zhu, D. Correlation analysis of PM$_{2.5}$ and O$_3$ in dry and rainy seasons in Hong Kong and Guangzhou from 2016 to 2021. *Fresenius Environ. Bull.* **2022**, *31*, 7877–7887.

49. Kutralam–Muniasamy, G.; Perez–Guevara, F.; Roy, P.D.; Elizalde–Martinez, I.; Shruti, V.C. Impacts of the COVID-19 lockdown on air quality and its association with human mortality trends in megapolis Mexico City. *Air Qual. Atmos. Health* **2021**, *14*, 553–562. [CrossRef]

50. Bert, B.; Maciej, S.; Jie, C.; Zorana, J.A.; Richard, A.; Mariska, B.; Tom, B.; Marie–Christine, B.; Jorgen, B.; Iain, C.; et al. Mortality and morbidity effects of long–term exposure to low–level PM$_{2.5}$, BC, NO$_2$, and O$_3$: An analysis of European cohorts in the ELAPSE project. *Res. Rep. (Health Eff. Inst.)* **2021**, *2021*, 208.

51. Zhang, T.; Wu, Y.; Guo, Y.; Yan, B.; Wei, J.; Zhang, H.; Meng, X.; Zhang, C.; Sun, H.; Huang, L. Risk of illness–related school absenteeism for elementary students with exposure to PM$_{2.5}$ and O$_3$. *Sci. Total Environ.* **2022**, *842*, 156824. [CrossRef] [PubMed]

52. Rashidi, R.; Khaniabadi, Y.O.; Sicard, P.; De Marco, A.; Anbari, K. Ambient PM$_{2.5}$ and O$_3$ pollution and health impacts in Iranian megacity. *Stoch. Environ. Res. Risk Assess. Res. J.* **2022**, 1–10. [CrossRef] [PubMed]

53. Zhou, X.S.; Liao, Z.H.; Wang, M.; Chen, J.; Zhao, X.; Fan, S. Characteristics of ozone concentration and its relationship with meteorological factors in Zhuhai during 2013–2016. *Acta Sci. Circumstantiae* **2019**, *39*, 143–153.

54. Song, X.; Hao, Y. Analysis of ozone pollution characteristics and transport paths in Xi'an city. *Sustainability* **2022**, *14*, 16146. [CrossRef]
55. Li, L.; Mao, Z.; Du, J.; Chen, T.; Cheng, L.; Wen, X. The impact of COVID-19 control measures on air quality in Guangdong province. *Sustainability* **2022**, *14*, 7853. [CrossRef]